

# Applications of LiDAR measurement for road management

Shinpei AKIYAMA\*and Masataka TAKAGI\*\*

Department of Infrastructure System Engineering

Kochi University of Technology

Tosayamada, Kochi, Japan

\*E-mail: [120285h@ugs.kochi-tech.ac.jp](mailto:120285h@ugs.kochi-tech.ac.jp)

\*\*E-mail: [takagi.masataka@kochi-tech.ac.jp](mailto:takagi.masataka@kochi-tech.ac.jp)

**ABSTRACT:** Since LiDAR (Light Detection And Ranging) is a suitable equipment for archiving three-dimensional surface data of any objects. Moreover, aerial LiDAR is used for the topographical survey, urban planning or forest measurement. On the other hand, ground based LiDAR has a potential for other purposes, such as landslide monitoring or landcover change monitoring. This paper reports method of landslide and landcover monitoring using LiDAR for road management.

Firstly, landslide monitoring technique using ground based LiDAR was developed. The amount of movements of a landslide should be precisely measured using LiDAR. In this study, Choja landslide in Japan was measured by LiDAR with a measurement accuracy of 6 mm. The result showed movement of landslide was detected in almost 1cm accuracy. An intersection point calculation of three surfaces was very effective for the accurate measurement. However, this technique can adapt for artificial object which include a plane. This method should be expand for natural objects such as natural slope or natural cliff.

Secondary, landcover change is also detected by ground based LiDAR. A wide area landcover should be classified automatically using LiDAR. The landcover change can be extracted by converting grid model and comparing the elevation of the objects. Vegetated areas are changing seasonally and annually. The land cover change was detected in Choja. The results showed agricultural land could be extracted. Classified trees and Rice fields showed higher accuracy. LiDAR also acquires RGB color information. The classification will improve by using RGB color information in near future.

**KEYWORDS:** Ground based LiDAR, Landslide monitoring, Landcover monitoring

## 1. Background

Since LiDAR (Light Detection And Ranging) is a suitable equipment for archiving three-dimensional surface data of any objects. Moreover, aerial LiDAR is used for the topographical survey, urban planning or forest measurement. On the other hand, ground based LiDAR has a potential for other purposes, such as landslide monitoring or landcover change monitoring.

In the landslide area, the ground is moving a few mm or a few cm per year. Therefore, accurate time series analysis is required to detect the displacement

of the landslide for conserving infrastructure.

For landcover monitoring, Change of the plant around a road must be detected for road conservation. Growth of trees makes disturb a visibility of a road.

## 2. Objectives

In this study, methodology of landslide monitoring and landcover monitoring will be established for road conservation.

In landslide monitoring, the amount of movements of a landslide should be precisely analyzed using LiDAR. In landcover monitoring, a wide area

landcover should be classified automatically using LiDAR.

### 3. Landslide Monitoring

Test area is Choja landslide in Japan. Choja landslide has occurred in about 200 m in width, and about 900 m in length. And this landslide is located on green schist area. Landslide observation by ground based LiDAR is carried out periodically in Choja area. Choja landslide is observed twice a year.

In this study, the downward edge of the landslide was measured by LiDAR. In addition, measurement targets were protection blocks which are constructed along the edge of landslide. 41 blocks were selected as the targets. Figure 3.1 showed target objects for the landslide monitoring.

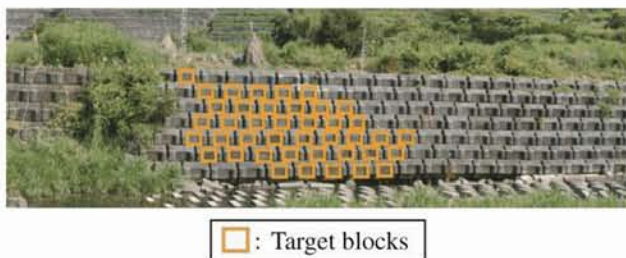


Figure 3.1 Monitoring Objects

#### 3.1 Used LiDAR

In Choja, landslide movement is 1~2 cm per year. Therefore, it is necessary to carry out precise measurement. So, LiDAR with a measurement accuracy of 6 mm was used in this research. Used LiDAR is Cyrax-2500 produced by Leica-Geosystems. Photo 3.1 showed appearance of Cyrax-2500. And Table 3.1 showed specification of Cyrax-2500. This LiDAR's effective measurement range is 100 m. And this LiDAR measurement field is narrow coverage.



Photo 3.1 Appearance of Cyrax-2500

Table 3.1 Specification of Cyrax-2500

Products of Laser Scanner	Cyrax-2500
Effective measurement range	2~100m
Measurement field	40°×40°
Ranging accuracy	±6mm
Measurement time	20 minutes

#### 3.2 Monitoring Method

LiDAR measurements were carried out on August 22, 2010 and August 19, 2011. Acquired LiDAR data are including random errors. According to the past research achievements, plane measurement performs high accuracy to reduce the random errors 1) 2) 3). The shape of the surface can be understood on LiDAR data. The outline of the landslide displacement extraction is shown Figure 3.2.

The first, three surfaces of a block is extracted from measurement data. The second, intersection point of three surfaces is calculated from the extracted data. The third, the geometric compensation of the intersection point is carried out. Finally, displacement will be detected.

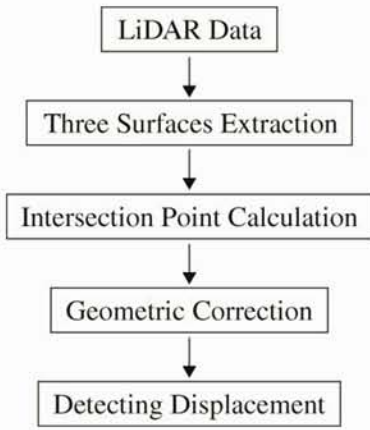


Figure 3.2 Monitoring method flow

The following equation shows a plane formula.

$$au + bv + cw = l$$

a,b,c,: Coefficients

u,v,w: Three-dimensional coordinates of acquisition data

The data on three surfaces of the block is extracted from the LiDAR data (Figure 3.3). A plane formula is derived and three coefficients were computed using the extracted three-dimensional coordinate data by least-squares method. The following equation shows the coefficient calculation by a least-squares method.

$$\begin{pmatrix} a \\ b \\ c \end{pmatrix} = \begin{pmatrix} \sum u_i^2 & \sum u_i v_i & \sum u_i w_i \\ \sum u_i v_i & \sum v_i^2 & \sum v_i w_i \\ \sum u_i w_i & \sum v_i w_i & \sum w_i^2 \end{pmatrix}^{-1} \begin{pmatrix} \sum u_i \\ \sum v_i \\ \sum w_i \end{pmatrix}$$

a,b,c,: Coefficients

u<sub>i</sub>,v<sub>i</sub>,w<sub>i</sub>: Three-dimensional coordinate of acquisition data

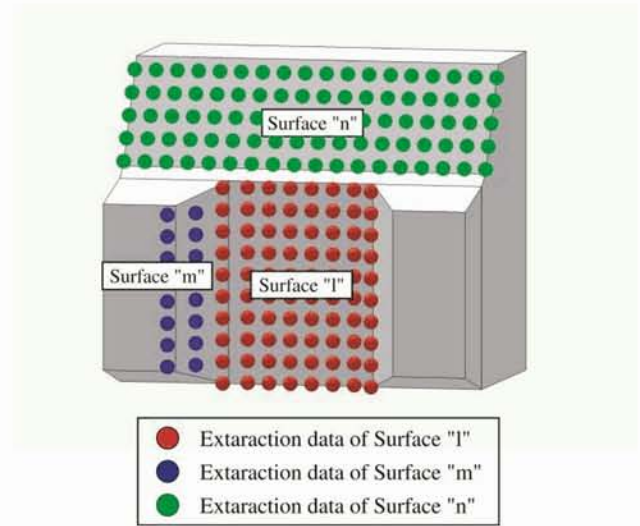


Figure 3.3 Surface extraction data

The intersection point is calculated from three surfaces. Figure 3.4 showed intersection point of a block. The following equation shows intersection point calculation.

$$\begin{pmatrix} u_p \\ v_p \\ w_p \end{pmatrix} = \begin{pmatrix} a_l & b_l & c_l \\ a_m & b_m & c_m \\ a_n & b_n & c_n \end{pmatrix}^{-1} \begin{pmatrix} l \\ l \\ l \end{pmatrix}$$

a<sub>l</sub>,b<sub>l</sub>,c<sub>l</sub>,: Coefficients of surface “l”

a<sub>m</sub>,b<sub>m</sub>,c<sub>m</sub>,: Coefficients of surface “m”

a<sub>n</sub>,b<sub>n</sub>,c<sub>n</sub>,: Coefficients of surface “n”

u<sub>p</sub>,v<sub>p</sub>,w<sub>p</sub>: Three-dimensional coordinate of intersection point

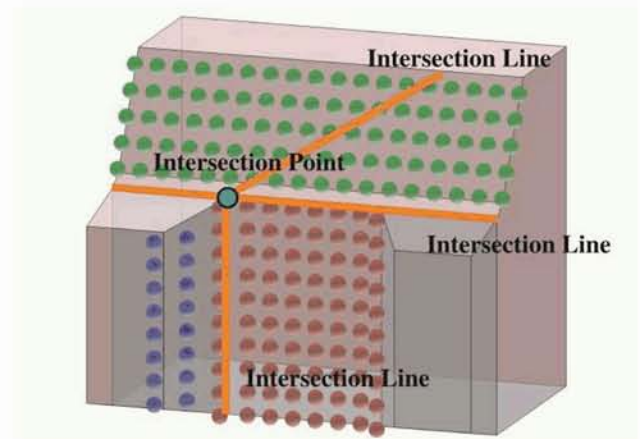


Figure 3.4 Intersection point of a block

In this study, LiDAR measurement was carried out on 2010 and 2011 to detect the displacement. Each LiDAR measurement data is not same coordinate system by setting error. Then, the geometric compensation is necessary to unified same coordinate system. Three-dimensional affine transform was applied for geometric compensation. As follows:

$$\begin{pmatrix} x_i \\ y_i \\ z_i \end{pmatrix} = \begin{pmatrix} p_0 & p_1 & p_2 \\ p_3 & p_4 & p_5 \\ p_6 & p_7 & p_8 \end{pmatrix} \begin{pmatrix} u_i \\ v_i \\ w_i \end{pmatrix} + \begin{pmatrix} x_0 \\ y_0 \\ z_0 \end{pmatrix}$$

$x_i, y_i, z_i$ ,: Three-dimensional ground coordinate  
 $u_i, v_i, w_i$ ,: Three-dimensional LiDAR coordinate  
 $x_0, y_0, z_0$ ,: Three-dimensional ground coordinate of LiDAR position  
 $p_0$ ~ $p_8$ : Conversion factors

The coordinate systems of the raw data acquired by LiDAR called LIDAR coordinates. The coordinate system after geometric compensation is transformed to a ground coordinate.

This transform requires four or more ground control points(GCP) to determine conversion factors. A ground control point means ground coordinates are known in LiDAR data. Six GCPs were used in this research. The following equation shows the geometric transformation calculation by a three-dimensional affine transform. Conversion factor and LiDAR position coordinate are computed by least-squares method. As follows;

$$\begin{pmatrix} p_0 \\ p_1 \\ p_2 \\ x_0 \end{pmatrix} = \begin{pmatrix} \sum u_i^2 & \sum u_i v_i & \sum u_i w_i & \sum u_i \\ \sum u_i v_i & \sum v_i^2 & \sum v_i w_i & \sum v_i \\ \sum u_i w_i & \sum v_i w_i & \sum w_i^2 & \sum w_i \\ \sum u_i & \sum v_i & \sum w_i & n \end{pmatrix}^{-1} \begin{pmatrix} \sum x_i u_i \\ \sum x_i v_i \\ \sum x_i w_i \\ \sum x_i \end{pmatrix}$$

$$\begin{pmatrix} p_3 \\ p_4 \\ p_5 \\ y_0 \end{pmatrix} = \begin{pmatrix} \sum u_i^2 & \sum u_i v_i & \sum u_i w_i & \sum u_i \\ \sum u_i v_i & \sum v_i^2 & \sum v_i w_i & \sum v_i \\ \sum u_i w_i & \sum v_i w_i & \sum w_i^2 & \sum w_i \\ \sum u_i & \sum v_i & \sum w_i & n \end{pmatrix}^{-1} \begin{pmatrix} \sum y_i u_i \\ \sum y_i v_i \\ \sum y_i w_i \\ \sum y_i \end{pmatrix}$$

$$\begin{pmatrix} p_6 \\ p_7 \\ p_8 \\ z_0 \end{pmatrix} = \begin{pmatrix} \sum u_i^2 & \sum u_i v_i & \sum u_i w_i & \sum u_i \\ \sum u_i v_i & \sum v_i^2 & \sum v_i w_i & \sum v_i \\ \sum u_i w_i & \sum v_i w_i & \sum w_i^2 & \sum w_i \\ \sum u_i & \sum v_i & \sum w_i & n \end{pmatrix}^{-1} \begin{pmatrix} \sum z_i u_i \\ \sum z_i v_i \\ \sum z_i w_i \\ \sum z_i \end{pmatrix}$$

n: Number of data

Table 3.2 showed accuracy of geometric compensation. The result of geometric compensation shows less than 6-mm error on 2010 and 2011. Therefore, displacement of over 1 cm can be detected.

Table 3.2 RMSError of geometric compensation

	X	Y	Z
2010 Summer	0.0029	0.0012	0.0032
2011 Summer	0.0037	0.0059	0.0044

### 3.3 Results

Landslide displacement was extracted by comparing the amount of movement of these intersection points. Figure 3.5 showed amount comparisons of movements (X-Y plane). And figure 3.6 showed amount comparisons of movements (Y-Z plane). Protection blocks moved maximum 2.6cm in the x axis direction, maximum 1.8cm in the y axis direction, maximum 3cm in the z axis direction.

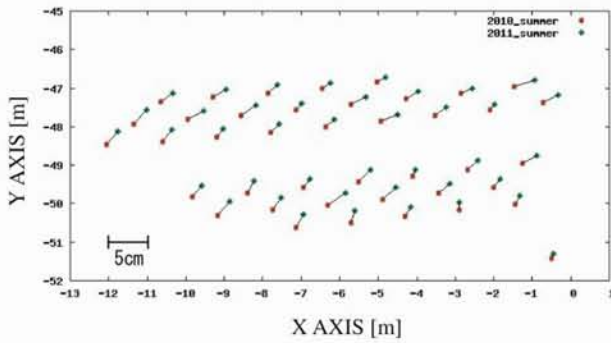


Figure 3.5 Amount comparisons of movements (X-Y plane)

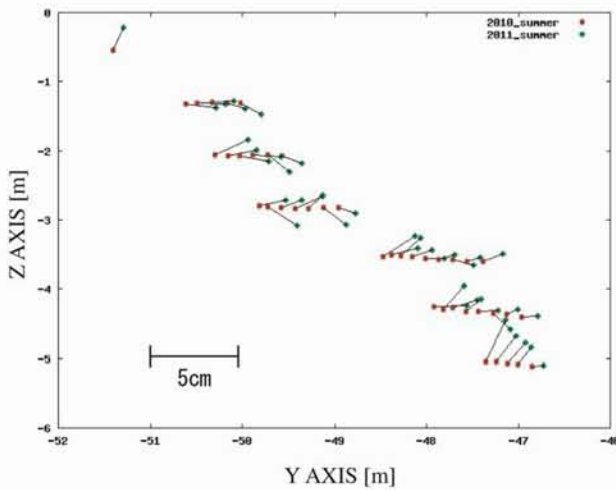


Figure 3.6 Amount comparisons of movements (Y-Z plane)

All blocks were moving along the direction of the landslide. Some blocks of the lower part were moved upward direction. It means uplift phenomenon on the edge of landslide. The result showed movement of landslide was detected in almost 1cm accuracy.

## 4. Landcover Monitoring

### 4.1 Used LiDAR

Landcover measurement requires wide range measurement. The accuracy should be lower than landslide monitoring. LiDAR has necessity which can acquire wide range data in a short time. So, LiDAR with effective measurement range of 350 m

and measurement field of  $80^{\circ} \times 333^{\circ}$  was used in this research. Used LiDAR is LMS-Z210 produced by Riegl. Photo 4.1 showed appearance of LMS-Z210. And Table 4.1 showed specification of LMS-Z210.



Photo 4.1 Appearance of LMS-Z210

Table 4.1 Specification of LMS-Z210

Products of Laser Scanner	LMS-Z210
Effective measurement range	2~350m
Measurement field	$80^{\circ} \times 333^{\circ}$
Ranging accuracy	$\pm 25\text{mm}$
Measurement time	15 minutes

### 4.2 Monitoring Method

LiDAR measurement was carried out on March 3, 2011 and August 19, 2011. Originally raw LiDAR data are represented by point cloud model which is based on 3D random point data. The first, point cloud data was converted into grid data. The grid size is 50 cm x 50 cm. Figure 4.1 showed general idea of conversion. In the case of high density data, many points are included on one pixel grid. Then, the maximum value and the minimum value of elevation on the grid are extracted from point cloud data. The minimum value means the ground surface, the maximum value means the top of the feature or vegetation.

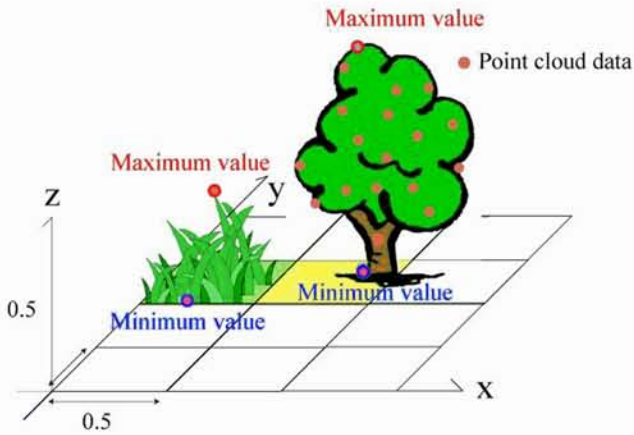


Figure 4.1 Converted grid data

The elevation value on the grid data is subtracted and change is extracted. The value which subtracted the minimum value of winter from the maximum value of winter is calculated. Figure 4.2 showed difference of elevation image (winter max value – winter min value). A road and a building are almost no change. A tree area or orchard area has overwhelmingly much change because of the height. The value which subtracted the maximum value of winter from the maximum value of summer is calculated. Figure 4.3 showed difference of elevation image (summer max value – winter max value). A rice field and a vegetable field have much change below 0.1 m ~ less 1.5 m.

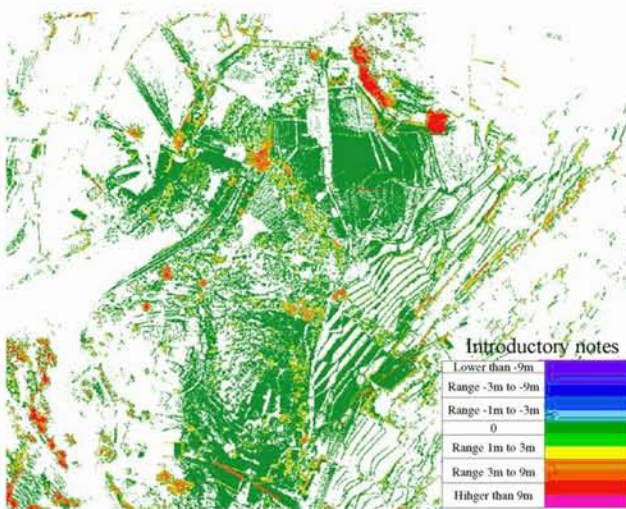


Figure 4.2 Difference of elevation image (Winter max value - winter min value)

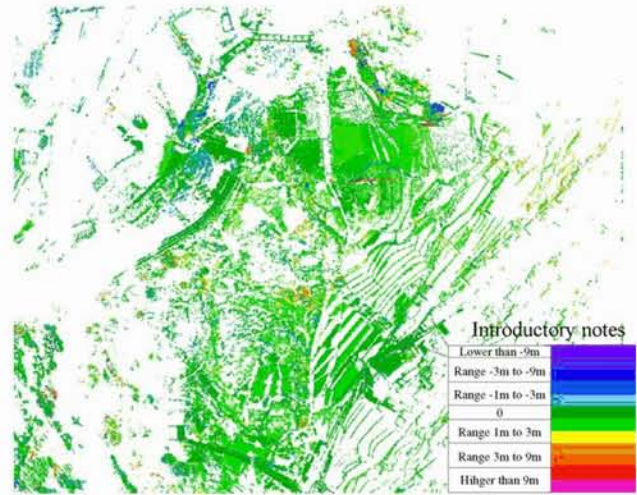


Figure 4.3 Difference of elevation image (Summer max value - winter max value)

Landcover classification in each grid is performed using decision tree algorithm. Figure 4.4 showed the algorithm. For example, if the difference of the maximum of winter and the minimum of winter shows higher than 2.5 m, then the grid assign into trees, else the grid classifies according to the difference of the maximum of summer and the maximum of winter. If the difference is lower than 0.1 m, then the grid assign into a road. If the difference ranges 0.1 m to 1.5 m, then the grid assign into rice field. If the difference is higher than 1.5 m, then the grid assign into wasteland.

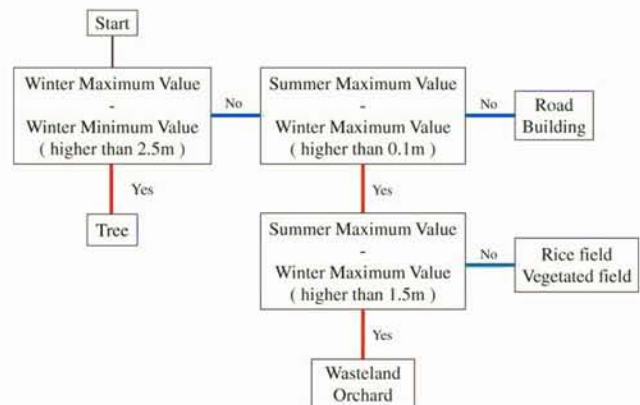


Figure 4.4 Decision tree algorithm

### 4.3 Results

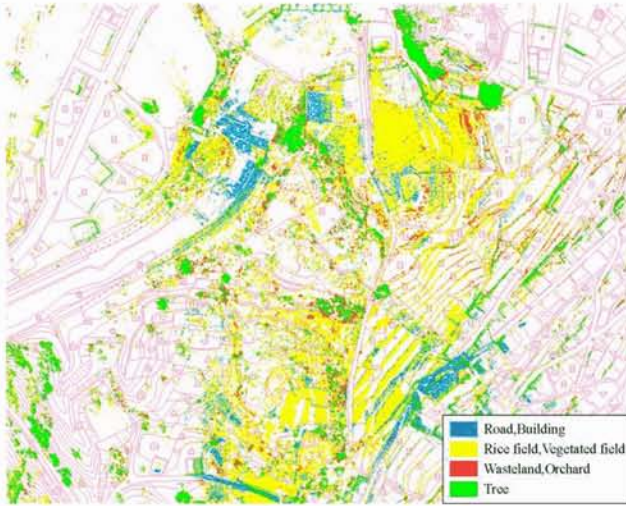


Figure 4.5 Classification result image

Figure 4.5 shows result of classification. For verification of a classification result, the land cover data was generated from map digitizing. The polygon for verification was classified into four, such as a building and a road, a rice field and a field, wasteland and an orchard, and trees, respectively. Figure 4.6 showed polygon for verification.



Figure 4.6 Polygon for verification

In order to compare the polygon for verification with a classification result, the concordance rate for every classification item was calculated. Table 4.2 showed the concordance rate.

Trees and Rice fields showed higher accuracy. Wasteland and an orchard, and a road and a building showed a lower.

Table 4.2 Concordance rate

	Concordance rate
Trees	79.3%
Rice field , Vegetated field	78.8%
Wasteland , Orchard	23.8%
Building , Road	47.8%

## 5. Conclusions

In this study, method of landslide and landcover monitoring using LiDAR was established. This time, movement of 41 protection blocks on landslide showed in almost 1cm accuracy. An intersection point calculation of three surfaces on the protection block was very effective for the accurate measurement. However, this technique can adapt for artificial object which include a plane. This method should be expand for natural objects such as natural slope or natural cliff.

In the landcover monitoring, the classification of a tree and a vegetated field showed high accuracy. LiDAR also acquires RGB color information. The classification will improve by using RGB color information.

Periodical LiDAR measurement will be very effective for road management.

## REFERENCES

- 1)R. Inada, M. Takagi, Displacement Detection of Landslide by using Ground Based LiDAR, Takagi Laboratory, Kochi University of Technology, 2010.
- 2)K. Kinoshita, M. Takagi, Accuracy Evaluation of Laser Scanner Data Depending on Location of GCPs for Monitoring Landslide, Takagi Laboratory, Kochi University of Technology, 2007.
- 3)T. Sakai, J.H. Jeong, and M. Takagi, Measurement Method of Landslide displacement with ground based portable laser scanner, Takagi Laboratory, Kochi University of Technology, 2006.